SUPPLEMENTARY MATERIALS

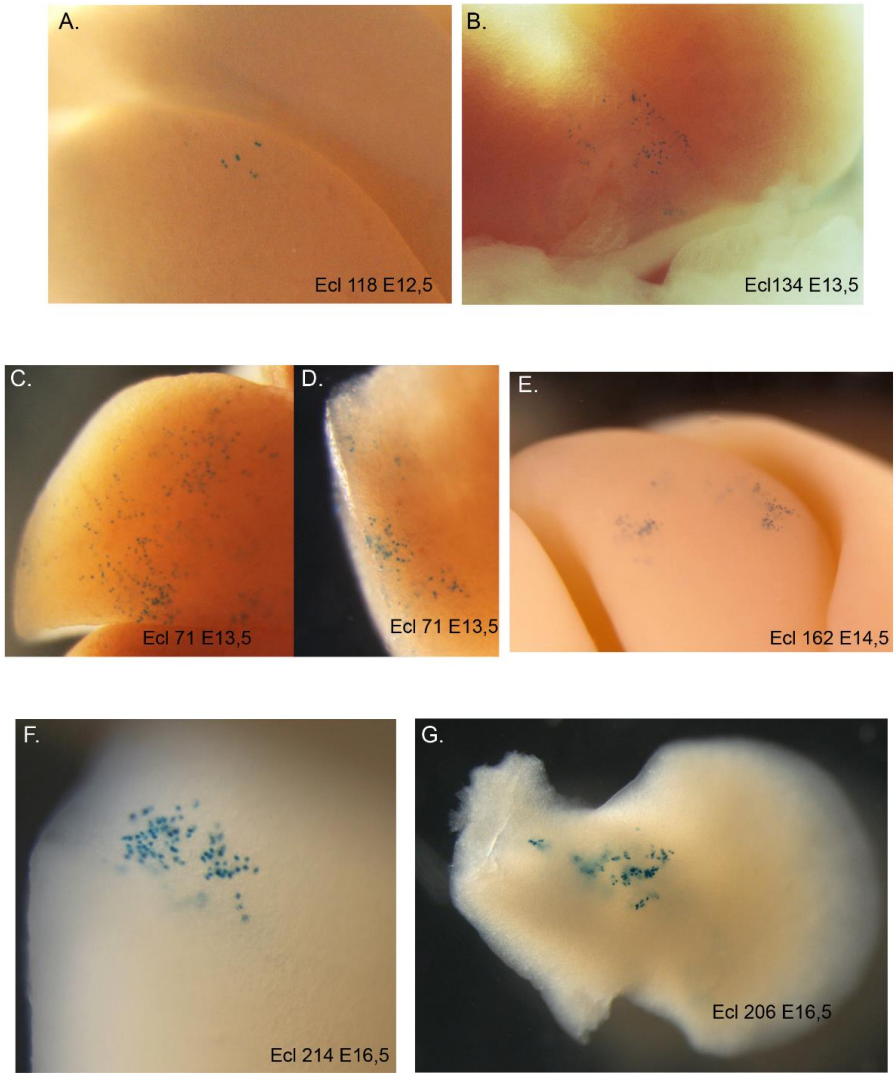

Fig. S1. **A**. Ecl 118 (E 12.5) shows 4 groups of 2 cells, located near the ventral wall of the LL lobe near to its meeting with the LM lobe. **B**. Ecl 134 (E13.5) where 136 blue nuclei can be counted using the microscope; these cells are located on the lower edge of the RM. **C, D**. Ecl 71 (E13.5) is particularly large (287 cells counted) and is seen both on the lateral (**C**) and caudal (**D**) surfaces of the LM. **E**. Ecl 162 (E14.5) occupies two areas of the RL comprising 182 cells. **F**. Ecl 214 (E16.5) is on the lateral edge of the caudate lobe, which emerges from and lies under the RL.**G**. Ecl 206 (E16.5) occupies nearly half of the newly emerging paddle-shaped papillary process, a very small lobe that develops on the central under side of both the left and right portions of the liver, but is derived from the RL. Stripes are present; 137 cells were counted. Lobe abbreviations: L, left or lateral; M, medial; R, right; C, caudate; PP, papillary process.

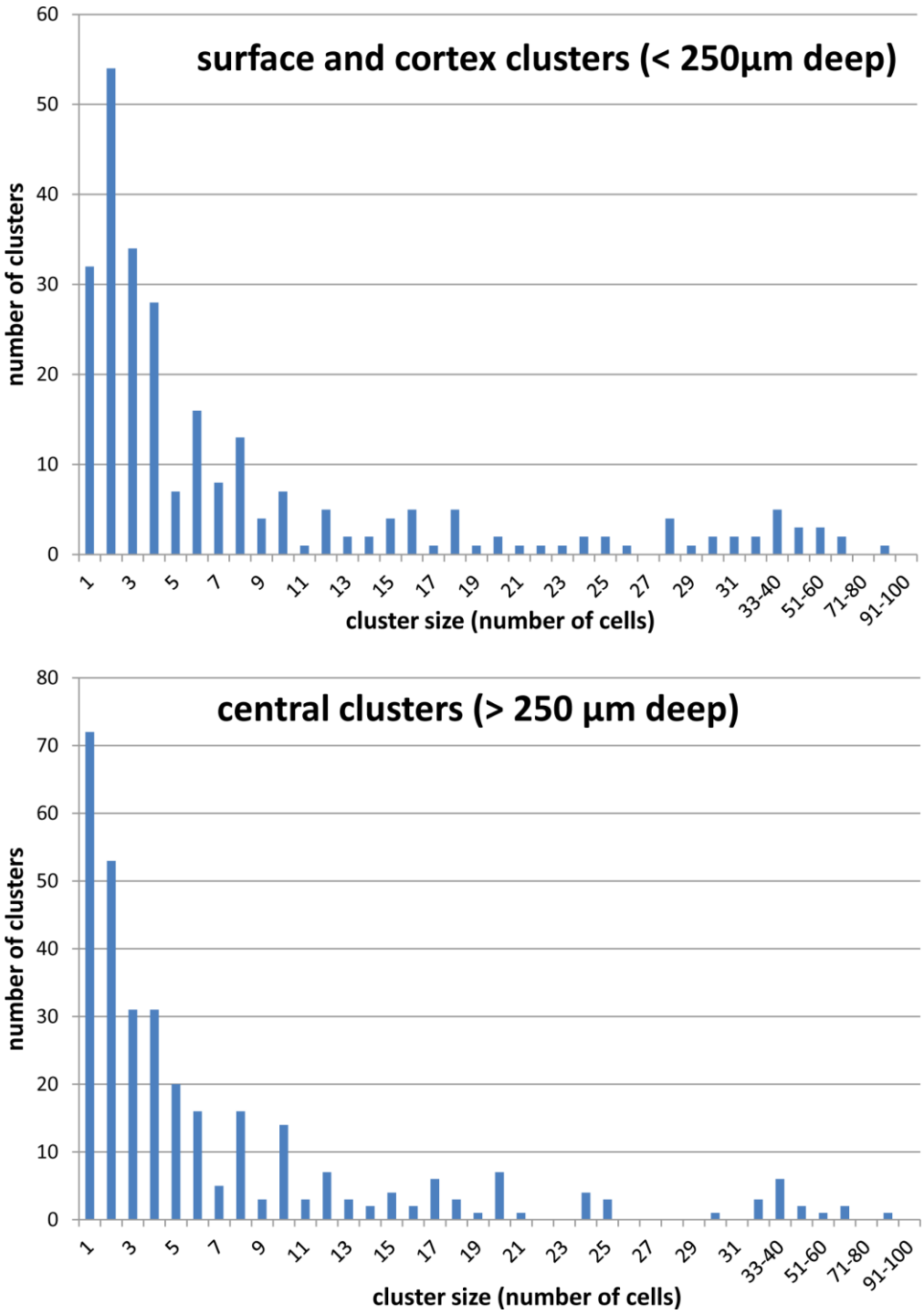

Fig. S2 Comparison of the frequency and size of clusters deep within the liver to those visible from the surface. All sections were counted, and the clusters were divided into two classes: those that were located at the surface and within 250-300µm of the surface, and those that were more deeply embedded within the section. The histograms depict the sizes of clusters and the numbers encountered either at/near the surface or deep within the section.

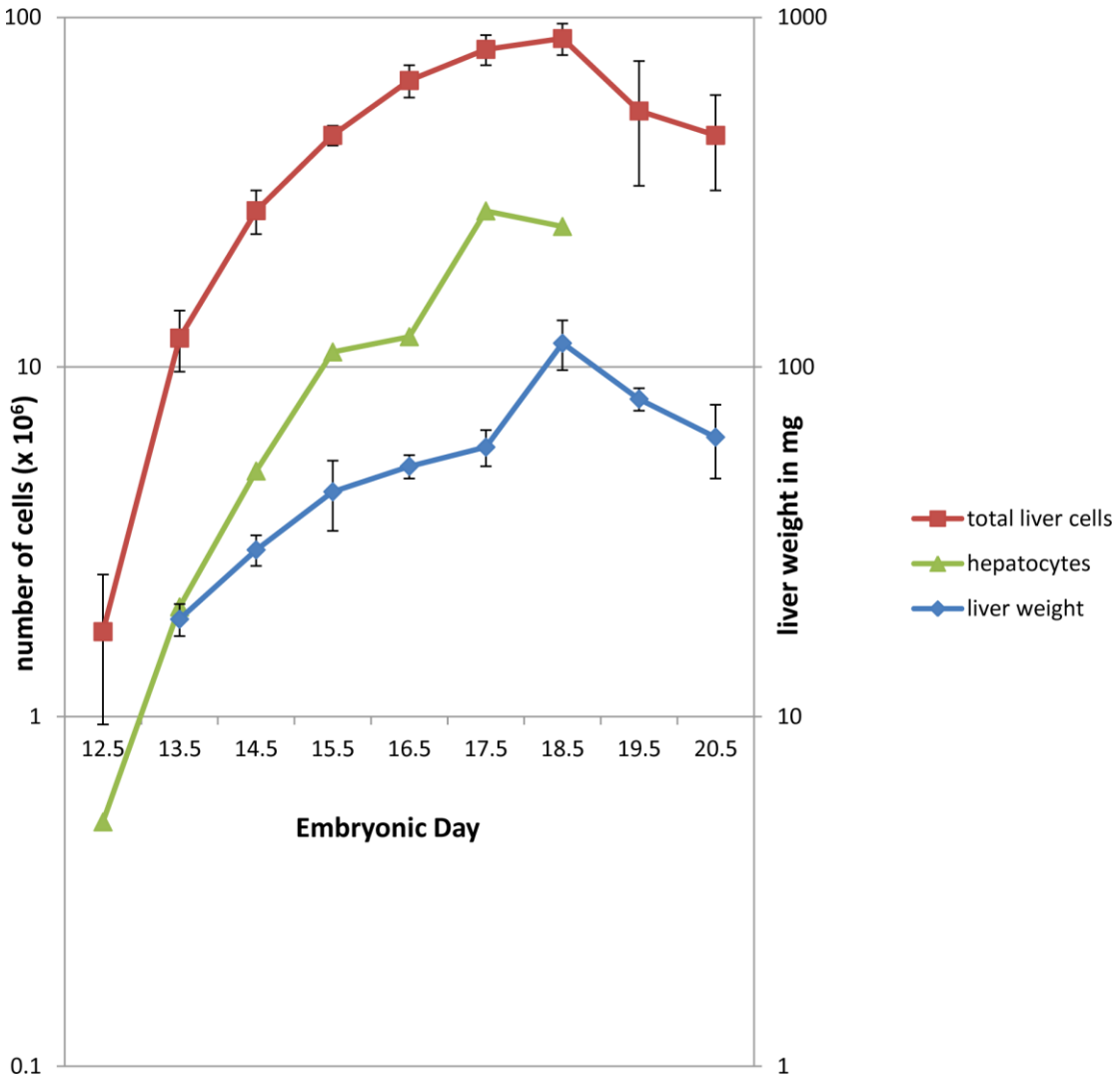

Fig. S3. Growth curves used to calculate average generation times during different phases of liver development. The values were calculated from tables presented in Paul et al., 1969 (Tables 1 and 2). Vassy et al. (1988) present a morphometric and stereological analysis of the developing rat liver between days 12 and 20: the volumetric fractions of hepatocyte nuclei permit us to plot the slope of hepatocyte growth, from which generation times can be deduced (Table 2 and embryonic liver weights given in the text). Three growth curves are shown: of total cells in the liver (squares), of hepatocytes (triangles), and weights of the embryonic livers (diamonds; scale in mg on the right).

Paul et al. (1969) counted total cells per liver using a trypsinized single-cell suspension of whole embryonic liver from E12.5 to E18.5 Swiss mice, and used cytocentrifugation and May-Grunwald Giemsa staining to prepare material for differential counts of the cell types. Liver weights were also determined. Vassy et al. (1988) have carried out stereological and morphometric analysis on livers of E12 to E18 Wistar rat embryos. The values of interest to us were total volumes of the livers and the volumetric fractions of hepatocyte nuclei (measured on electron micrographs), which permitted us to establish the slope of the nuclear increments with time on a logarithmic scale. This avoided the necessity of correcting for increase in the cytoplamsmic volume of hepatoblasts/hepatocytes during development. The slopes obtained from data of Vassy etl al. (1988) were very similar to those of counts of hepatocytes by Paul et al. (1969), after correction for the developmental stage of E days for the rat compared to the mouse (Kaufman, 1992). The slopes for the rat are not shown in the figures because of the differences in timing of development of the two species.

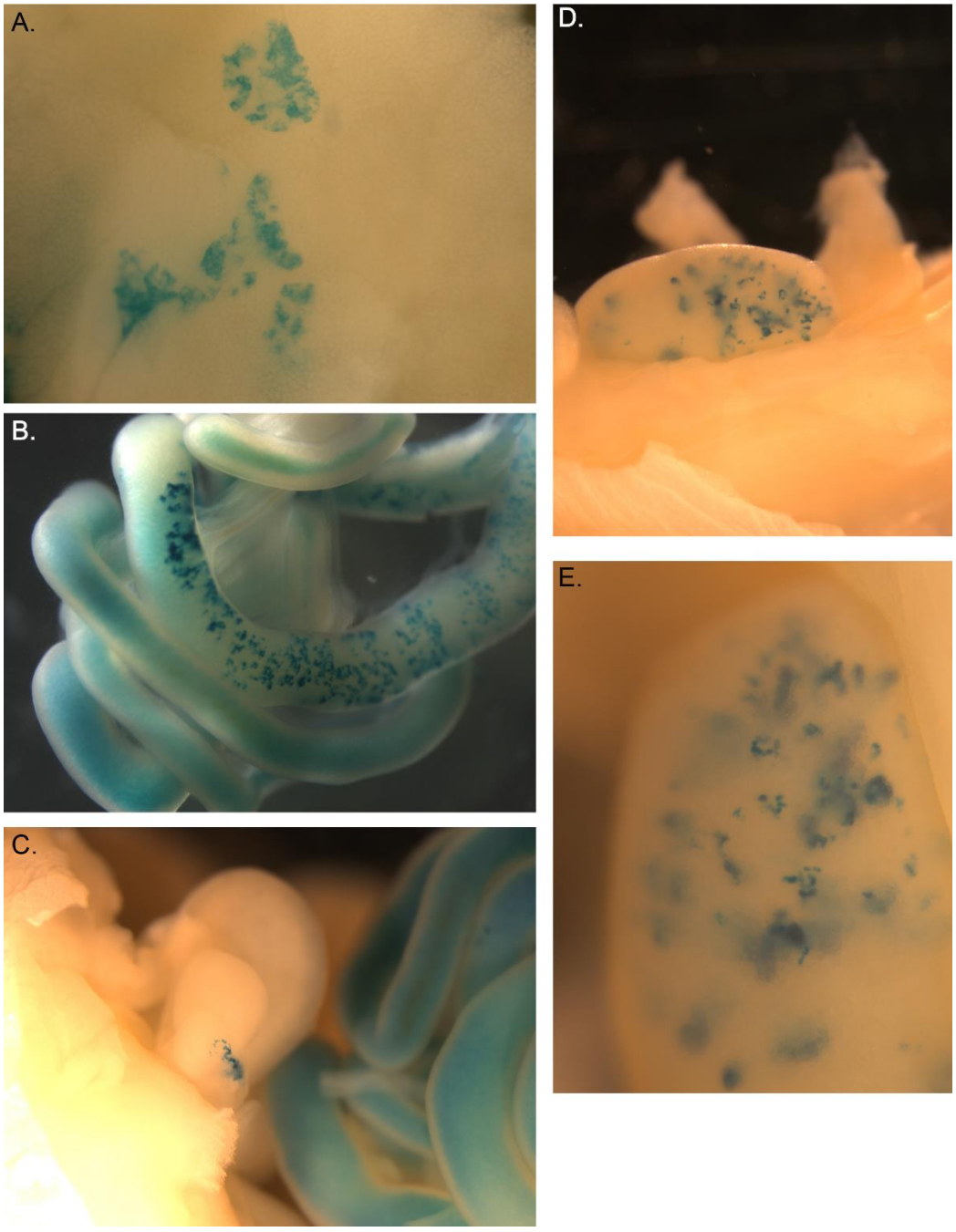

Fig. S4. Labeled clusters in non-liver tissues that express HNF4α. A. Pancreas (40X), 3 week old mouse. B. Large intestine (E 17.5 embryo); 8X C. Testis (E16.50; the labeled tissue is the epidydimus (8X). D and E. Kidney (E16.5) (8X and 25X respectively). The convoluted tubules contain HNF4α.